Using Match Uncertainty in the Kalman Filter for a Sonar Based Positioning System

Oddbjørn Bergem, Claus Siggaard Andersen, Henrik Iskov Christensen
Norwegian Defence Research Establishment, Norway
Laboratory of Image Analysis, Aalborg University, Denmark

ABSTRACT

Much effort has been devoted to computer vision methods for navigation and tracking of flights, cars, robots, and autonomous vehicles. Less work has addressed the problems of visual navigation under water, which is the topic of this paper. We present a method for incorporating the uncertainty of the matching between a model of the sea floor and measurements, obtained with a multibeam sonar, in a Kalman filter. The technique is based on using second order centralised moments in a region of interest to estimate the measurement uncertainty/error. This error is then used to calculate the measurement covariance matrix in the Kalman filter. We provide experimental results on real data to show that this method is superior to the standard Kalman filter in which the measurement error covariance matrix typically is set constant or varies deterministically.

1. Introduction

Navigation has always been an interesting area for researchers. Recently, there has been considerable interest in using computer vision for navigation of flights [4,7], cars [12], and autonomous land vehicles and robots [3,6,10]. For navigation in an underwater environment, less work has been reported. Even if the demand for such systems is high, the low visibility in water leads to very specialised systems restricted to operate close to an object or near the sea floor [9]. An example of such a system is described in [1], which computes the relative movement of the AUV (Autonomous Underwater Vehicle) by extracting and matching features in successive pictures. Another example is described in [5], where an AUV follows pipelines based on visual information. To overcome the problems of low visibility, we are working on a system based on a multibeam sonar which is directed toward the sea floor. A multibeam sonar may be thought of as N sonars connected in a one-dimensional array with a fixed angle between the beams. Instead of returning one depth measurement, the multibeam sonar returns a vector containing N depth measurements. A picture of an AUV using a multibeam sonar is showed in figure 1.1. For details of the underlying mathematics and beam forming techniques the reader is referred to [11] .

Figure 1.1 Multibeam sonar

In navigation two approaches may be used: Relative navigation or absolute navigation, where the latter approach uses landmarks to remove incremental errors. When using multibeam sonars, candidates for landmarks are profiles of the sea floor. Obviously this will not give a unique global position for every measurement independent of the underlying sea floor structure, but if the sea floor has a minimum of variation, we show in section 5 that the information of the sea floor profile combined with a predict-match-update schema implemented with a Kalman filter, give sufficient information for navigation purposes.

A crucial concern in the design of the system is how to incorporate information in the prediction filter. In vision based navigation systems, the measurements are normally deduced from a match between the sensor data and the underlying model data. However, additional information exists from the matching process which can be used to estimate the measurement noise. Based on this idea, we show in section 4 how the error between the data and the model in a region of interest easily can be used to update the measurement covariance matrix to dynamically represent the actual uncertainty of the measurement. We show in section 5 examples with real data where this information is essential for the filter to return to the correct track.

2. Probabilistic estimation - The Kalman filter

The Kalman filter is a least square estimation technique using a Bayesian approach. The filter is used to track the state of stochastic dynamic systems being observed with noisy sensors. Essentially, the filter is based on three separate probabilistic models. The first model describes the evolution over (discrete) time by the equation

$$\mathbf{x}(k+1) = \mathbf{F}(k)\mathbf{x}(k) + \mathbf{G}(k)\mathbf{u}(k) + \mathbf{v}(k) \qquad (2.1.)$$

where $\mathbf{x}(k)$ is the state at time k, $\mathbf{u}(k)$ is the controlled input signal entering the system with gain matrix $\mathbf{G}$, and $\mathbf{v}(k)$ is a sequence of zero-mean white Gaussian process noise with covariance matrix $\mathbf{Q}(k)$. $\mathbf{F}$ is the transition matrix of the system.

The second model describes the measurement, and relates the measurement vector $\mathbf{z}$ to the current state through a measurement matrix $\mathbf{H}$:

$$\mathbf{z}(k) = \mathbf{H}(k)\mathbf{x}(k) + \mathbf{w}(k) \qquad (2.2.)$$

Here $\mathbf{w}(k)$ is assumed to be a sequence of zero-mean white Gaussian noise with covariance

$$\mathbf{E}\left[\mathbf{w}(k)\mathbf{w}^T(j)\right] = \mathbf{R}(k)\delta_{kj} \qquad (2.3.)$$

where δ_{kj} is the Kronecker delta. The third model describes the knowledge about the system state and its covariance before the first measurement is taken. Usually the initial system state is assumed to be a normally distributed random variable with a known mean and a given covariance matrix:

$$\mathbf{x}(0) \sim \mathbf{N}\left[\hat{\mathbf{x}}(0|0), \mathbf{P}(0|0)\right] \qquad (2.4.)$$

where $\mathbf{P}$ is the associated conditional state error covariance matrix and the vector $\hat{\mathbf{x}}(a|b)$ is the conditional state estimate.

So far we have only set up the equations for the models of a system. The one step prediction stage can be calculated using the formula

$$\hat{\mathbf{x}}(k+1|k) = \mathbf{F}(k)\hat{\mathbf{x}}(k|k) + \mathbf{G}(k)\mathbf{u}(k) \qquad (2.5.)$$

where the prediction is calculated by applying the transition matrix $\mathbf{F}$(k) to the previous state estimate and adding the control input. The system state estimate may be calculated by the formula

$$\hat{\mathbf{x}}(k+1|k+1) = \mathbf{F}(k)\hat{\mathbf{x}}(k|k) + \mathbf{W}(k+1)\left[\mathbf{z}(k+1) - \mathbf{H}(k+1)\hat{\mathbf{x}}(k+1|k)\right] \qquad (2.6.)$$

This shows that the new estimate, using the measurement $\mathbf{z}$(k+1), is formed by extrapolating the estimated vector, and then adding a correction term. This correction term, called the innovation (or measurement residual), is formed by subtracting the predicted measurement vector from the new observation vector $\mathbf{z}$(k+1). The gain matrix $\mathbf{W}$ contains information of how much the innovation should affect the new state estimate. In a Kalman filter, the gain is related recursively to the covariance matrix $\mathbf{P}$(k+1|k) by the formula

$$\mathbf{W}(k+1) = \mathbf{P}(k+1|k)\mathbf{H}^T(k+1)\mathbf{S}^{-1}(k+1) \qquad (2.7.)$$

where $\mathbf{S}^{-1}(k+1)$ is given by

$$\mathbf{S}(k+1) = \mathbf{H}(k+1)\mathbf{P}(k+1|k)\mathbf{H}^T(k+1) + \mathbf{R}(k+1) \qquad (2.8.)$$

The state prediction covariance matrix is

$$\mathbf{P}(k+1|k) = \mathbf{F}(k)\mathbf{P}(k|k)\mathbf{F}^T(k) + \mathbf{Q}(k) \qquad (2.9.)$$

and the updated state covariance matrix is

$$\mathbf{P}(k+1|k+1) = \mathbf{P}(k+1|k) - \mathbf{W}(k+1)\mathbf{S}(k+1)\mathbf{W}^T(k+1) \qquad (2.10.)$$

The area where the matching algorithm search for a match between the model and the data is called the validation gate [2]. The validation gate V is related to the inverse of the prediction covariance matrix $\mathbf{S}$ and the innovation. It describes an ellipse in the

measurement space and is the minimum volume that contains a given probability mass under the Gaussian assumption. The validation gate is defined as:

$$V_{k+1}(l) \equiv \left\{ \mathbf{z} : \left[\mathbf{z} - \hat{\mathbf{z}}(k+1)|k) \right]^T \mathbf{S}^{-1}(k+1) \left[\mathbf{z} - \hat{\mathbf{z}}(k+1)|k) \right] \le l \right\} \tag{2.11.}$$

$$= \left\{ \mathbf{z} : \mathbf{v}^T(k+1)\mathbf{S}^{-1}(k+1)\mathbf{v}(k+1) \le l \right\} \tag{2.12.}$$

The innovation $\mathbf{v}$ that defines the validation gate is chi-square distributed with number of degrees of freedom equal to the dimension of the measurement vector $\mathbf{z}$ [2]. With dim($\mathbf{z}$) = 2 setting $l = 4$ results in 86% of the probability mass inside the validation gate.

For a deeper description of the Kalman filter refer to [2].

3. System description

Our system may be described by the discrete time, linear system equation

$$\mathbf{x}(k+1) = \mathbf{F}\mathbf{x}(k) + \mathbf{v}(k) \tag{3.1.}$$

with the measurement equation

$$\mathbf{z}(k) = \mathbf{H}\mathbf{x}(k) + \mathbf{w}(k) \tag{3.2.}$$

as the matrices $\mathbf{F}$ and $\mathbf{H}$ are time invariant, and there is no known input to the system (see equation 2.1 and 2.2). The system state vector contains the position in Cartesian coordinates together with the velocities:

$$\mathbf{x}(k) = \begin{bmatrix} x(k) & \dot{x}(k) & y(k) & \dot{y}(k) \end{bmatrix}^T \tag{3.3.}$$

From the multibeam sonar and the matching process we calculate the measured position:

$$\mathbf{z}(k) = \begin{bmatrix} x_m(k) & y_m(k) \end{bmatrix}^T \tag{3.4.}$$

The state transition matrix $\mathbf{F}$ for our constant velocity system is

$$\mathbf{F} = \begin{bmatrix} 1 & T & 0 & 0 \\ 0 & 1 & 0 & 0 \\ 0 & 0 & 1 & T \\ 0 & 0 & 0 & 1 \end{bmatrix} \tag{3.5.}$$

where T is the sampling period. The measurement matrix $\mathbf{H}$ is

$$\mathbf{H} = \begin{bmatrix} 1 & 0 & 0 & 0 \\ 0 & 0 & 1 & 0 \end{bmatrix} \tag{3.6.}$$

Because we operate with a global coordinate system, it is reasonable to assume that the axis directions are symmetric. This is also true for the velocity. The system covariance matrix is then

$$\mathbf{Q} = \begin{bmatrix} \sigma_m^2 & 0 & 0 & 0 \\ 0 & \sigma_v^2 & 0 & 0 \\ 0 & 0 & \sigma_m^2 & 0 \\ 0 & 0 & 0 & \sigma_v^2 \end{bmatrix} \tag{3.7.}$$

4. Estimation of the measurement covariance matrix

The term $\mathbf{w}(k)$ represents measurement noise related to the sensor, including any matching uncertainty and lack of confidence in a specific measurement. The covariance matrix for the measurement noise thus contains contributions both from sensory noise and from the matching process. If the terrain has much structure, it is likely that a unique and confident match can be determined, but in flat terrain the uncertainty in the matching process increases caused by many possible matches. In a hillside, one typically will have considerable uncertainty in the position in one direction and low uncertainty in the other direction. As a consequence, it is necessary to account for such uncertainties in the covariance matrix for the measurement error. To accomplish this the matching strength matrix for the validation gate is analysed.

Define the area W to be the smallest rectangular area which contains the validation gate V. For each location in W, a measurement strength $fv(x, y)$ akin to the idea of a correlation type of matching is computed. There are three restrictions on $fv(x, y)$:

$$fv(x, y) = 0 \quad if \quad (x, y) \notin V \tag{4.1.}$$

$$fv(x, y) \geq 0 \quad \forall (x, y) \in V \tag{4.2.}$$

$$\sum_{x,y} fv(x, y) = 1 \tag{4.3.}$$

From equation 4.2 and 4.3 we see that $fv(x, y)$ has the properties of a distribution.

If the position corresponding to the best match (x_c, y_c) is used as the reference position, it is possible to calculate centralised statistical moments for the area W. If first and second order moments are calculated, information that specifies the confidence in the

5

match is available. These moments provide an estimate of the covariance matrix $\mu(k)$ associated with the match:

$$\mu(k) = \begin{bmatrix} \mu_{20}(k) & \mu_{11}(k) \\ \mu_{11}(k) & \mu_{02}(k) \end{bmatrix} \qquad (4.4.)$$

The second order statistic is calculated using the general formula for central statistical moments:

$$\mu_{pq} = \sum_x \sum_y fv(x,y)(x-x_c)^p(y-y_c)^q \qquad (4.5.)$$

From equation 4.5 we see that small values on the moments will indicate a very certain match, while high values on the moments correspond to the situation where multiple strong matches are present in the validation gate.

We now combine the matrix $\mu(k)$ with the sensor noise covariance matrix to generate the new measurement covariance matrix $\mathbf{R}(k)$:

$$\mathbf{R}(k) = \mu(k) + \mathbf{N} = \begin{bmatrix} \mu_{20}(k) & \mu_{11}(k) \\ \mu_{11}(k) & \mu_{02}(k) \end{bmatrix} + \begin{bmatrix} n_x & 0 \\ 0 & n_y \end{bmatrix} \qquad (4.6.)$$

where μ_{pq} are the second order centralised moments, and n_x and n_y are the variances due to noise in the sensors. Note that this matrix is time varying, and not constant or deterministic as in the Standard Kalman filter, as it at every time step will depend on the results from the actual matching process.

From the above equations it is evident that the measurement covariance matrix $\mathbf{R}$ will depend on the matching function $fv(x,y)$. This is a desirable property, because the matching function $fv(x,y)$ defines the matching strength between the different matches in the validation region, and therefore contains information about the measurement uncertainty.

In Kalman filtering, the measurement noise is assumed to be modelled as a zero-mean white noise Gaussian sequence. Analyses have been carried out that address the consequences of wrong assumptions in the process and measurement noise, and we refer to [8] for details. We are currently working on a post analysis of the behaviour of the measurement covariance matrix $\mathbf{R}$ in equation 4.6, and preliminary results are in a reasonable accordance with the assumptions.

5. Experimental results

The experiments use data recorded in a $1200m^2$ area from the cost outside Ålesund (western part of Norway). A 3D plot of the area is shown in figure 5.1. Figure 5.2 shows the two test tracks superimposed on a contour map of the area.
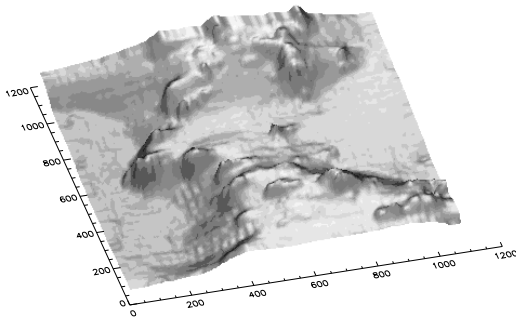
Figure 5.1 3D terrain map
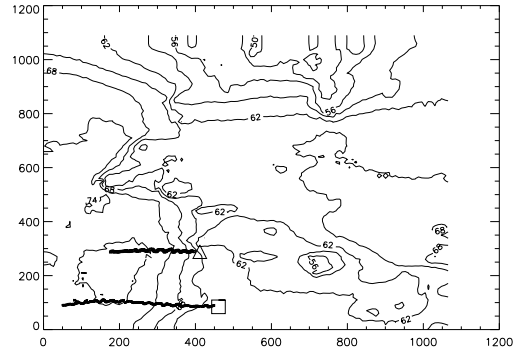
Figure 5.2 Contour map

The depth varies between 55 and 75 meters, and the area contains both flat and undulating parts. The terrain model was generated from west-east scan lines recorded with approximately 25% overlap. For measuring the correct positions a differential GPS was used, which under the recording conditions had an accuracy of approximately 4.0 meter. The multibeam sonar was an EM 100 from Simrad with 27 beams and 3.75° between each beam. For a depth of 60 meter this gives a viewing area of 105 meter between the outer beams. Both the model and the measurement data are recorded from a surface ship.

Figure 5.3 shows the error in x and y position for the lower track in figure 5.2. This track consists of 250 measurement done in 149 seconds, with a total distance of approximately 400 meters.
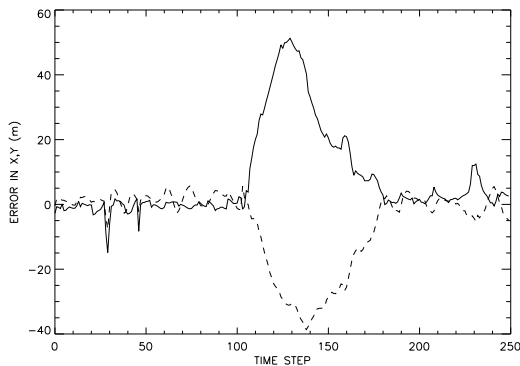
Figure 5.3. Error in x-solid and y.
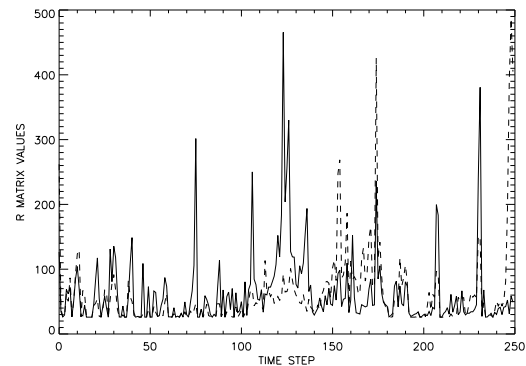
Figure 5.4. $\mathbf{R}$ (0,0)-solid and $\mathbf{R}$(1,1)

At time step 110, the algorithm enters the flat area in front of the hillside, and gets an error in x and y position. When reaching the hillside at time step 135, the algorithm enters a wrong valley (seen at the 3D map in figure 5.1 at position (340,140)), resulting in an error of 52 and 38 meter in the x and y position respectively. Locally this valley is now the best possible choice, but looking at the measurement covariance matrix in figure 5.4, we see that the matching results in high measurement uncertainty, and the algorithm is able to return to the correct track.

To show the improvement over the standard Kalman filter with fixed measurement covariance matrix $\mathbf{R}$, we run both filters on the higher track (marked with a triangle in

7

figure 5.2). This track consists of 160 measurements with many "traps" where the matching algorithm easily heads in a wrong direction. The filters where equal except for the measurement covariance matrices **R**. Figure 5.5 and 5.6 show the error in x and y for both filters. As seen in the figures, the standard Kalman filter is not able to return from the error, and looses the track. We have tried the standard filter with many different **R** matrices, but we have not been able to find values for **R** where the filter is able to follow
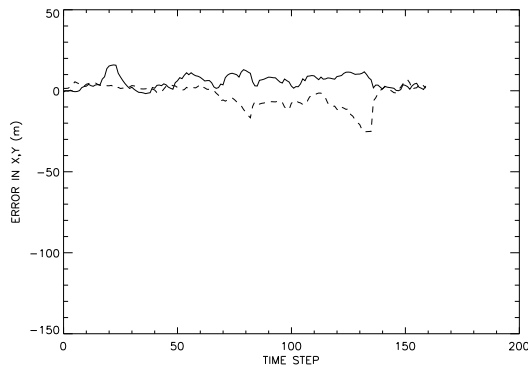
Fig. 5.5 Error in x-solid and y. **R** varying.
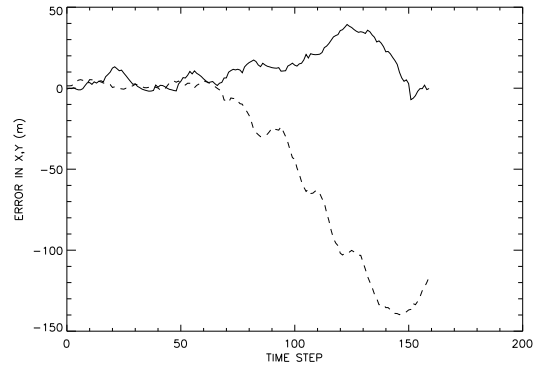
Fig. 5.6 Error in x-solid and y. **R** constant.

the tracks.

One explanation is immediate: If **R** is too large, the validation gate is forced large. Besides increasing the computational load, this causes the matching algorithm to search for a match in a large area, which easily results in a temporary better solution. Especially in "sine shaped" areas this has a fatal consequence. A large **R** will also decrease the system gain **W**, which in turn will suppress the measurements. If **R** is chosen too small, the standard Kalman filter fails because the filter then lacks the ability to return from local errors. Using the **R** matrix in equation 4.6 the validation gate will vary according to the uncertainty between the sensor measurement and the underlying terrain as seen in figure 5.7, and the filter is able to handle more difficult situations without loosing the track. An example of the gate error function used to compute **R** is shown in figure 5.8.
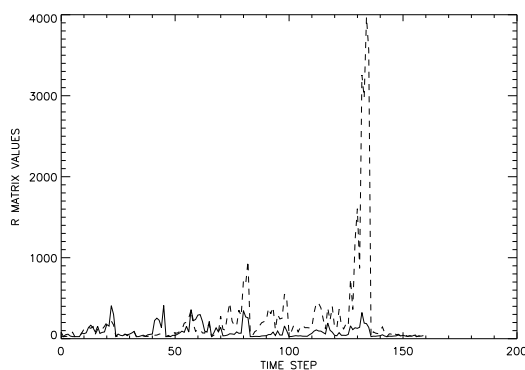
Fig. 5.7 **R** (0,0)-solid and **R**(1,1)
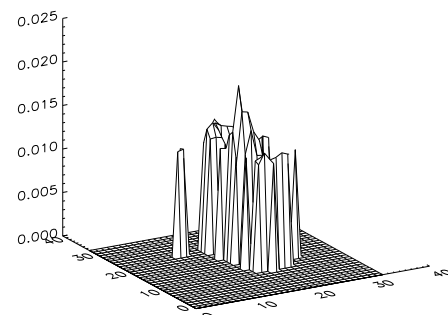
Fig 5.8 Example of gate error function.

6. Conclusion

We have developed a technique that easily incorporates uncertainty in the matching process when using a Kalman filter for navigation or tracking purposes. The technique uses second order moments in the validation gate to estimate the measurement error, resulting in a measurement covariance matrix varying dynamically according to the underlying model and data. Experiments from data recorded at the west cost of Norway indicate important improvements compared to a Kalman filter which uses a deterministic measurement covariance matrix. The improvements are mainly a consequence of using all accessible information about the match between model and data to give a correct assessment of the measurement error.

REFERENCES

[1.] F. Aguirre, J. M. Boucher, J.J.Jack, "*Underwater navigation by video sequence analysis*", Proc. 10th ICPR, Atlanitc City, USA, 1990.

[2.] Y. Bar-Shalom, T. E. Fortmann. "*Tracking and Data Association*", Academic Press,1988.

[3.] I. J. Cox, "*Blanche:Position Estimation for an Autonomous Robot Vehicle*", Autonomous Robot Vehicles, Springer-Verlag, 1990.

[4.] E. Hagen, E. Heyerdahl, "*Navigation by optical flow*", Proc. 11th ICPR, Hague, Netherlands,1992.

[5.] J. O. Hallset, "*A Vision System for an Autonomous Underwater Vehicle*", Proc. 11th ICPR, Hague, Netherlands,1992.

[6.] A. Matthew et al, "*VITS-A Vision System for Autonomous Land Vehicle Navigation*", PAMI, May 1988.

[7.] J. J. Rodriguez, J. K Aggerwal, "*Matching Aerial Images to 3-D Terrain Maps*", PAMI, December 1990.

[8.] S. Sangsuk-Iam, T. E. Bulloc. "*Analysis of Discrete-Time Kalman Filtering Under Incorrect Noise Covariances*", Tr. on Automatic Control, December 1990.

[9.] S. Svendson, B. Ericson, "*Underwater vision*", FOA Report B 30243-3.1, Forsvarets Forskningsanstalt, S-581 Lindkøping, Sweden,1991.

[10.] C. Thorpe et al, " *Vision and Navigation for the Carnegie-Mellon Navlab*", PAMI, May 1988.

[11.] R. J. Urick, "*Principles of Underwater Sound*", 3rd edition, NcGraw-Hill, 1983.

[12.] T. Zielke, M. Brauckmann, W. von Seelen, "*Intensity and Edge-Based Symmetry Detection Applied to Car-Following*", Proc. ECCV, Santa Margherita Ligure, Italy, 1992.